SDSS'Rio 2010 STABILITY AND DUCTILITY OF STEEL STRUCTURES
E. Batista, P. Vellasco, L. de Lima (Eds.)
Rio de Janeiro, Brazil, September 8 - 10, 2010

DUCTILE RESPONSE OF COMPOSITE STEEL AND CONCRETE FRAMES

L. Di Sarno*

* Deparment of Engineering, University of Sannio, Benevento, Italy
e-mail: disarno@unina.it

Keywords: Composite steel and concrete frames, ductility, overstrength, inelastic response.

Abstract. *This analytical work investigates the ductile response of composite steel and concrete framed buildings subjected to horizontal earthquake loading. A code-compliant six-storey spatial moment resisting frame (MRF) was employed as sample structure. Nonlinear static and dynamic analyses were performed on a detailed three-dimensional finite element model of the benchmark system. Two models were employed for structural steel and steel reinforcement bars, namely elasto-perfectly plastic (EPP) and elasto-plastic with 2% hardening (EPH). Parametric section analyses were utilized to assess the variation of the section ductility and flexural overstrength with regard to the level of axial load. The outcomes of the performed analyses showed that for low values of adimensionalized axial load, i.e. Nsd/Nplrd < 0.10, the response parameters of the composite cross-sections are similar in terms of rotational ductility. However, as the axial loads increase the EPH model provides higher values of ductility compared to EPP counterparts. Global system overstrength was estimated to determine the level of plastic flexural redistribution occurring in the sample composite MRF. The design system overstrength (αu/α1) provided by the European and Italian seismic Code underestimates significantly the actual values of the ratio αu/α1; the values estimated for the benchmark structure vary between 2.65 and 3.07. As a result the MRF system possesses enhanced plastic redistribution and hence global energy absorption and dissipation. Furthermore, the sample code-compliant composite frame exhibits sufficient storey ductility as shown by the computed values of inter-storey drifts at collapse limit states.*

1 INTRODUCTION

Moment resisting frames (MRFs), especially in structural steel and reinforced concrete (RC), are often utilized as effective lateral resisting structural system in regions with high seismic risk world-wide. Composite steel and concrete structures tend to combine the beneficial effects of both steel and RC systems; the latter systems are cost-efficient especially for medium-to-high rise buildings. Composite beam-columns and joints possess adequate stiffness, strength and ductility to withstand gravity and earthquake-induced horizontal loads, e.g. [1]. Analytical studies and experimental tests addressing performance assessment of composite building frames are, however, still scarce [2, 3, 4]. Furthermore, local and global limit states to evaluate quantitatively the performance of composite systems are rarely specified in a detailed manner [5], both in numerical and experimental studies. On the other hand, seismic design provisions were recently implemented in international and national codes of practice for this type of lateral resisting systems, e.g. [6, 7, 8], among many others. Notwithstanding, only a limited number of studies have assessed the reliability and the degree of conservatism, if any, of the rules formulated in the novel design standards. The present analytical work assesses the earthquake response of a composite steel and concrete MRF building with six-storey and designed in compliance with recent national seismic standards [8]. Detailed static and dynamic (inelastic) analyses were employed to investigate the structural performance of the benchmark multi-storey building. The results of the inelastic pushovers are discussed herein. The response criteria were expressed in terms of plastic hinge rotations and inter-storey drifts.

2 SEISMIC DESIGN RULES

The current seismic standards formulated for the analysis and design of composite steel and concrete MRFs, especially in Europe [6, 8], were chiefly derived from the experimental and numerical simulations carried out on structural steel earthquake resistant systems. For example the all-encompassing behaviour factor q (R-factor in the US practice) utilized to estimate the design (inelastic) base shear by scaling down the elastic seismic demand, is the same for both bare steel and composite structures. There is sufficient recent evidence (e.g. [9; 10, 11], among others), however, that the q-factor, which accounts for the energy dissipation and absorption, should assume higher values for composite structures because of the enhanced local and global ductility, member overstrength and increased inherent structural damping. The effective confinement effect of concrete to inhibit local buckling should give rise to less stringent limitations for the slenderness ratios for I- and H-shaped sections. Partial strength shear connections, particularly at beam-to-column connections should be further investigated. The inherent damping of such connections and the reduced flexural capacity of the composite beams may result beneficial for enhanced performance within the capacity design framework. Additionally, capacity design rules, especially those relative to connections, beam-to-column and base columns, should validated through experimental tests. The existing provisions appear extremely conservative and uneconomic thus endangering the use of composite MRFs in seismic areas.

3 CASE STUDY

3.1 General Description

The sample office building structure assessed in this analytical work includes a structural system with 6-storey, and 5-bay and 4-bay moment resisting frame (MRFs); the MRFs are placed along the perimeter of the symmetrical plan layout. The bay lengths are 7.0m (two exterior bays), 6.0m (two intermediate bays) and 5.0m (central bay). The interstorey height is 3.5m for all but the ground floor, which is 4.0m high. The total height of the building is 21.5m.

The earthquake-resistant MRFs employ partially-encased composite columns; the cross-sections include hot rolled profiles: HEB400 (lower storeys) and HEB360 (upper storeys). The steel beams are IPE360 and IPE 330 (primary beams); IPE240 and IPE 270 are utilised as secondary beams. The floor system is a 120mm thick composite slab; the metal profiled sheeting is a A55/P600 Hi-Bond. The composite action between the steel beam and the metal profiled sheeting slab is guaranteed by Nelson-type shear studs (ductile shear studs); their height is 90mm and the diameter is 14 mm; ultimate strength fu=360N/mm2. The shear connection is a full-strength. The beam-to-column and column-to-base connections of the MRFs are full-strength and rigid.

The structural steel of beams and columns in the sample MRFs is grade S235 (fy=235MPa). The concrete used for the composite slab is normal weight (type C25/20); the design resistance is 11.0 N/mm2. A secant Young modulus was assumed for concrete; its estimated value is 29,962 N/mm^2. The steel bars used for the longitudinal and transverse reinforcement in the columns and for the mesh of the slabs are B450C with a design stress of N/mm^2. Material partial safety factor (γ_c) for concrete is assumed equal to 1.5, while values of γs equal to 1.05 and 1.15 are used for structural steel and for rebars and meshes, respectively.

The self-weight loads G_k are 4.67 kN/mq for all floors; the live loads Q_k are 2.00 kN/mq because of the type of occupancy of the building. The force partial safety factors γ_g and γ_q at the ultimate limit state (ULS) are 1.3 and 1.5, respectively. At serviceability limit state (SLS) the above factors are γ_g=γ_q=1.0. It is assumed that the building is located at 135m above the sea level and hence the load due to the snow is 0.48 kN/mq; the wind pressure is 0.85 kN/mq (windward) and 0.43 kN/mq (leeward).

The earthquake design of the sample frame was carried out by utilizing 5% damped acceleration response spectra at the ultimate (ULS) and serviceability (SLS). The spectra were computed at damageability limit state (DLS) and life safety (LSLS). The structure is located in an area of high

seismicity, near Naples, in the South of Italy; the estimated bedrock accelerations are 0.083g (SLS) and 0.258g (LSLS). The soil is type B (360m/s<vs,30<800m/s) and hence the site amplification factor S=1.2 at DLS and 1.162 at LSLS. The behaviour factor is q=6.50 (multi-storey MRF with multiple bays).

3.2 Numerical Model

The MRFs of the sample building structure were modelled through a three-dimensional finite element (FE) system consisting of elastic beam-elements with lumped plasticity hinges at both ends; the numerical model was implemented in the software SAP 2000 [12]. Each composite beam was discretized using 5 beam elements to model adequately the effective widths.

Beam-to-column connections are modelled as rigid joints and the column-to-base connections are assumed fully restrained. The non linear behaviour of concrete was modelled through the constitutive relationship formulated by [13] for monotonic load and reversal loads. Such relationship accounts for the different degree of confinement of the concrete in partially-encased columns and beams with profiled sheeting slab. Two models were also employed for the steel of the reinforcement bars: elasto-plastic and elasto-plastic with hardening**.**

The inelastic response of steel structural members was modelled by means of bilinear elasto-plastic and elasto-plastic with hardening stress-strain curves. For both models the deformation at yield is ε_{sy} = 0,002, the ultimate deformation ε_{su} = 0,02. It is assumed that, for the elasto-plastic with hardening model, the ultimate strength fsu=336 N/mm^2, which corresponds to a ratio E/Eh = 37,5 at the deformation ε= 0,02. For the columns, three different levels of concrete confinement were accounted for: fully confined (hourglass shape), partially confined (parabola shape) and unconfined (thin rectangular cover).The ultimate deformation of concrete was assumed equal to 0.5%. The deformation at the peak compressive strength f'c is 0.2%.

4 SYSTEM RESPONSE

4.1 Local Response

Comprehensive parametric analyses were carried on composite steel and concrete partially encased columns. Such analyses were aimed at establishing the effects of the non linear models (i.e. EPP and EPH) utilized for structural steel on the flexural behaviour. Additionally, the normalized level of axial load, i.e. N_{sd}/N_{plrd}, was varied between 0 (pure flexure) and about 0.25 (high axial load). Tables 1 and 2 provide the outcomes of the performed analyses for the HEB400 columns for the EPP and EPH model, respectively. The bending moments at yield (M_y), at collapse (M_u) and peak point (M_{max}) were computed along with the yield (X_y) and ultimate (X_u) curvatures**.** It is found that for low values of adimensionalized axial loads, i.e. $N_{sd}/N_{plrd} < 0.10$, the response parameters of the composite cross-sections are similar in terms of rotational ductility. However, as the axial loads increase the EPH provide higher values of ductility, e.g. $X_u/X_y = 4$ (EPP) versus $X_u/X_y = 9$ (EPH). The flexural overstrength, herein estimated as M_{max}/M_y, is for EPH model on average 20% higher than the EPP counterparts.

The abrupt reduction of the rotation ductility is found for values of $N_{sd}/N_{plrd} > 0.10$ (N=750kN); for the latter case, the results of the performed analyses show that the ductility is halved with respect to the case of pure flexure ($N_{sd}/N_{plrd} = 0$). These results do no depend on the numerical model employed for simulating the response of steel. Additionally, sudden post-peak loss of stiffness was detected for values of adimensionalized axial loads greater than 0.20 (N>1250kN), especially when EPP models are used. The bending moment-curvature diagrams for different levels of axial load for HEB400 column are pictorially displayed in Figure 1 for HEB400, with either EPP or EPH models.

N [KN]	Nsd/Nplrd	My [KNm]	Mu [KNm]	Mmax [KNm]	Xy [1/m]	Xu [1/m]	Ductility X_u/X_y	Overstrength M_{max}/M_y
0	0.00	705	959	962	0.0052	0.0894	17	1.37
250	0.04	757	921	981	0.0057	0.0963	17	1.30
500	0.07	780	913	985	0.0060	0.0963	16	1.26
750	0.11	816	920	987	0.0064	0.0688	11	1.21
1000	0.15	841	859	988	0.0070	0.0606	9	1.18
1250	0.19	858	960	987	0.0076	0.0275	4	1.15
1500	0.22	873	976	976	0.0083	0.0225	3	1.12

Table 1 – Section analysis results of HEB 400 columns with different level of axial load (EPP model).

N [KN]	Nsd/Nplrd	My [KNm]	Mu [KNm]	Mmax [KNm]	Xy [1/m]	Xu [1/m]	Ductility X_u/X_y	Overstrength M_{max}/M_y
0	0.00	716	1229	1229	0.0054	0.0962	18	1.72
250	0.04	762	1229	1229	0.0057	0.0962	17	1.61
500	0.07	785	1221	1221	0.0060	0.0962	16	1.56
750	0.11	815	1209	1209	0.0064	0.0865	13	1.48
1000	0.15	849	1210	1210	0.0070	0.0774	11	1.43
1250	0.19	851	1137	1137	0.0075	0.0687	9	1.34
1500	0.22	860	1099	1099	0.0081	0.0606	7	1.28

Table 2 – Section analysis results of HEB 400 columns with different level of axial load (EPH model).

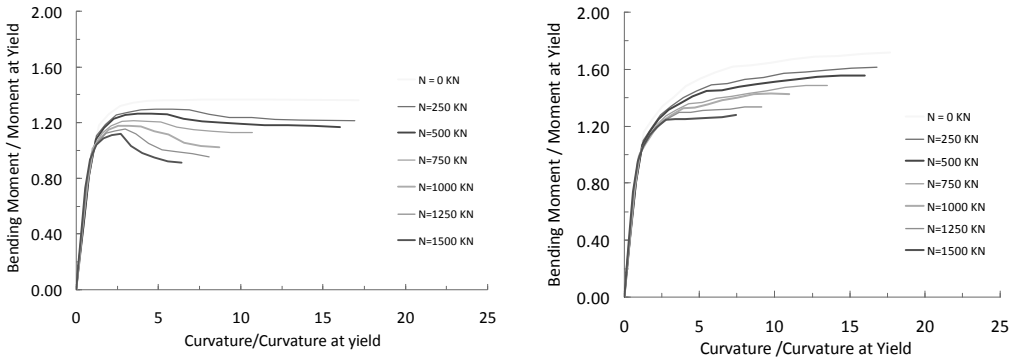

Figure 1 – Bending moment-curvature diagram for differen levels of axial load for HEB400 column: EPP (left) and EPH (right).

The above findings were also derived for the partially encased HEB360 members. It can thus be argued that the FE structural models based on EPP formulations tend to underestimate the effective energy dissipation capacity of the composite members, thus engandering the reliable assessment of the seismic structural performance. he variations of the rotation ductility and flexural overstrength with the level of axial loads are displayed in Figure 2 for elasto-perfectly plastic and elasto-plastic with hardening models. For the latter model the response tend to be independent of the cross-section type. The rotational ductility and flexural overstrength exhibit a linear decreasing trend as the normalized axial load N_{sd}/N_{plrd} increases. The regression analyses of the computed values shown a high correlation with the linear trend; the R^2-factor are closed to the unity.

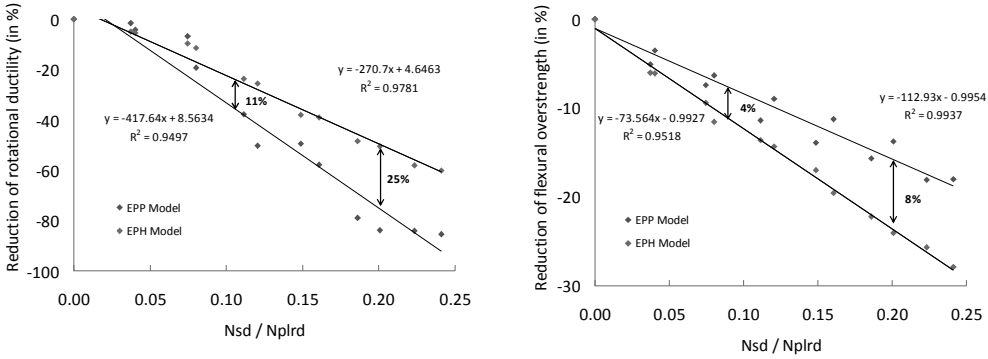

Figure 2 – Variation of ductility (left) and flexural overstrength (right) for partially encased column using EPP and EPH models with respect to the case of N=0.

The outcomes of the extensive parameter analyses prove that the rotation ductility is reduced by about 10% for low values of adimensionalized load, e.g. N_{sd}/N_{plRd} =0.10, and 25% for high values of the ratio N_{sd}/N_{plRd}. The variation of flexural overstrength ranger between 4% and 8% and is not significant for practical applications. The results of the parameter analyses demonstrate that the EPP models tend to understimate the plastic energy dissipation of columns with moderate-to-high level of axial loads. This is the case, for example, of base columns in MRFs, where plastic hinges (dissipative zones) are localized to achieve full plastic collapse mechanism under earthquake lateral loads. The results estimated for EPH models are characterized by lower reduction of rotation ductility as a function of the axial load because the hardening tends to redistribute within the member cross-section the material inelasticity. As a result, the inelastic deformation of the section is augmented.

4.2 Global Response

The modal response of the sample frame was first investigated; the fundamental period of vibration is 2.13 seconds along X-direction and 2.05 seconds along Y-directions. The effective modal mass associated to the above modes is 82%. The estimated natural period of vibration is 1.87 seconds; this value is significantly larger that those computed through simplified expressions implemented in modern seismic codes of practice [7, 8, 9]. However, lower values of the period provide conservative estimate of the design forces.

The inelastic performance of the sample composite framed building was assessed through inelastic static analyses (pushovers). Two load patterns were employed: uniform and inverted triangular. The computed

capacity curves are shown in Figure 3 for X- and Y-directions. The onset of the code-compliant limit states, i.e. damageability (DLS), life safety (LSLS) and collapse (CPLS), is also estimated. The structural response was derived by utilizing both the EPP and EPH models. The onset of collapse is detected by the ultimate rotation of the plastic hinges. For the EPP models the collapse is reached at a drift of about 2.5% along X-direction and 2.2% along Y-direction. The lateral inelastic deformation is not significantly affected by the load pattern distribution. The estimated top roof lateral drifts at collapse are lower when the EPH model is utilized, e.g. 1.96% versus 2.54% for X-direction and inverted triangular load pattern. The results of the inelastic static analyses provided in Figure 3 show that the largest variations are detected along the X-direction, where the number of bays (and hence plastic hinges) is higher. The inelastic response of the benchmark MRF was also assessed in terms of inter-storey drift (d/h), which can be utilized as an effective measure of structural and non-structural damage of MRF structures. The latter drifts were computed at different code-compliant limit states, namely DLS, LSLS and CPLS. It is found that the onset of the ultimate rotation capacity (see Figure 3) corresponds to values of inter-storey drifts higher than 3%, i.e. 4.0% and 3.5% along X- and Y-direction, respectively.

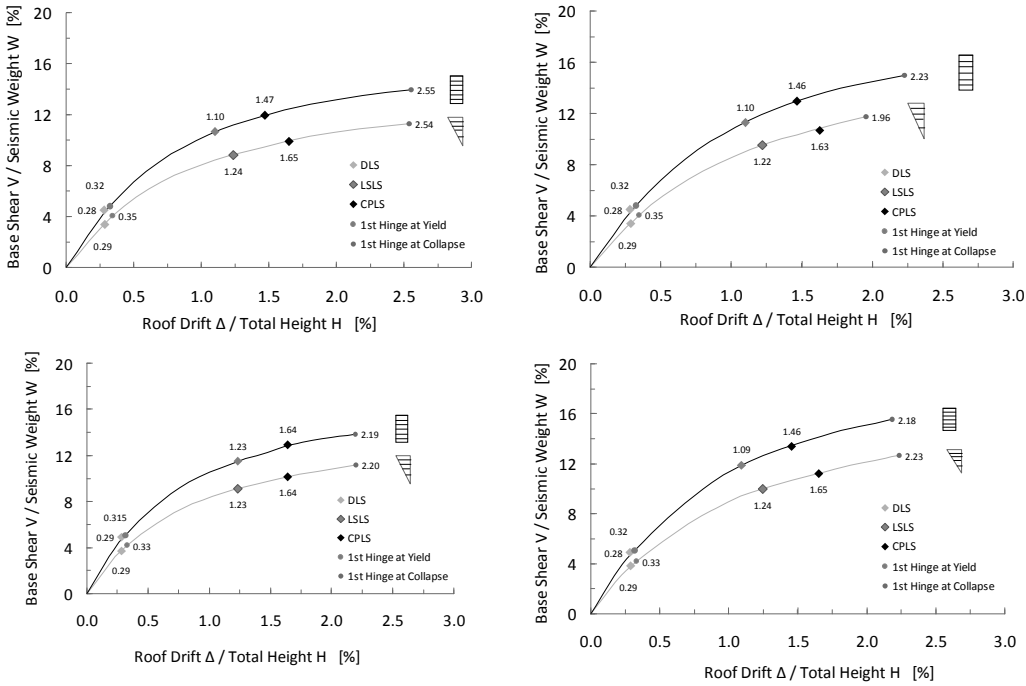

Figure 3 – Capacity curves along the X (left) and Y-direction (right) using EPP (top) and EPH (bottom) models.

The outcomes of the inelastic pushovers also demonstrate that the EPH model leads to higher strength capacity and lower deformation demands. The values of global translation ductility μ and system overstrength α_u/α_1 are summarized in Table 4 for EPP and EPH models, for inverted triangular and uniform load patterns, X- and Y-directions.

	ELASTIC PERFECTLY PLASTIC				*ELASTO-PLASTIC WITH HARDENING*			
Seismic Input Direction	X		Y		X		Y	
Seismic Load Pattern	Triang	Unif	Triang	Unif	Triang	Unif	Triang	Unif
Ductility μ	7.3	7.9	6.6	7.0	5.7	5.5	6.7	6.7
System overstrength α_u/α_1	2.78	2.90	2.90	2.65	2.89	2.90	3.01	3.07

Table 4 – System translation ductility and overstrength.

The computed values show that the q-factors that was utilized for the design of the sample composite frame, i.e. q=6.50, is close to those derived through inelastic static analyses. The global translation ductility μ varies between 5.5 and 7.9; thus, the average value is consistent with the design q-factor. However, the system overstrength as specified in the European seismic codes of practice ([6], [8]) are significantly lower than those computed with FE numerical models. The upper bound of the code values for the ratio α_u/α_1 is 1.3; the estimated values range between 2.65 and 3.07. It can be argued that the actual plastic redistribution of the composite steel and concrete MRF systems is significantly underestimated in the current design standards.

6 CONCLUSIONS

The results of the present analytical study show that the mechanical model employed for the steel, especially structural steel, can influence significantly the response parameters of the inelastic behaviour of composite steel and concrete multi-storey moment resisting frame (MRF). Two models were considered herein, i.e. elasto-perfectly plastic (EPP) and elasto-plastic with 2% hardening (EPH). It is found that for low values of adimensionalized axial load, i.e. Nsd/Nplrd < 0.10, the response parameters of the composite cross-sections are similar in terms of rotational ductility. However, as the axial loads increase the EPH models provide higher values of ductility compared to EPP counterparts. Inelastic static (pushover) analyses were carried out to derive capacity curves and to assess the structural performance in terms of both local (plastic rotations) and global (inter-storey drifts) response quantities. The outcomes of the performed inelastic analyses showed that the design system overstrength (αu/α1) provided by the European and Italian seismic Code underestimates significantly the actual values of the ratio αu/α1; the values estimated for the sample structure vary between 2.65 and 3.07. As a result composite MRF systems possess enhanced plastic redistribution and hence global energy dissipated**.** Further analytical and experimental tests are deemed necessary to assess the reliability of the existing code rules and to promote the use of composite steel and concrete structures, especially MRF, in earthquake-prone areas.

REFERENCES

[1] Nakashima, M., Matsumiya, T., Suita, K. and Zhou, F. (2007). Full scale test of composite frame under large cyclic loading. *Journal of Structural Engineering*, ASCE, 133(2), 297-304.

[2] El-Tawil, S. and Deierlein, G.G. (2001). Nonlinear Analysis of Mixed Steel-Concrete Frames. II: Implementation and Verification. *Journal of Structural Engineering*, ASCE, 127(6), 656-665.

[3] Spacone, E. and El-Tawil, S. (2004). Nonlinear analysis of steel-concrete composite structures: State of the art. *Journal of Structural Engineering*, ASCE, 130(2), 159-168.

[4] Zhoul, F., Mosalam, K.M. and Nakashima, M. (2007). Finite-Element Analysis of a Composite Frame under Large Lateral Cyclic Loading. *Journal of Structural Engineering*, ASCE, 133(7), 1018-1026.

[5] Broderick, B.M. and Elnashai, A.S. (1996). Seismic response of composite frames - I. Response criteria input motion. *Engineering Structures*, 18(9), 696-706.

[6] Eurocode 8 (2004). Design provisions for earthquake resistance of structures. Part 1.3: General rules. Specific rules for various materials and elements. Eur. Comm. for Standardisation, Brussels, Belgium.

[7] American Institute of Steel Construction (2005). Seismic Provisions for Structural Steel Buildings. Chicago, IL, USA.

[8] DD.MM.LL.PP. (2008). Norme tecniche per le costruzioni - NTC (*in Italian*).

[9] Plumier A., Doneux C. editors. (2001). Seismic Behaviour and Design of Composite Steel Concrete Structures. ISBN 972-49-1890-4. LNEC Edition. Lisbon.

[10] Thermou, G.E., Elnashai, A.S., Plumier, A. e Doneux, C. (2004). Seismic design and performance of composite frames. Journal of Constructional Steel Research, 60(1), 31-57.

[11] Bursi, O.S., Caramelli, S., Fabbrocino, G., Molina, J., Salvatore, W., Taucer, F., (2004). 3D Full-scale seismic testing of a steel-concrete composite building at ELSA. Contr. No. HPR-CT-1999-00059, European Community.

[12] Computer and Structures (2008), *SAP2000 Integrated Finite Element Analysis and Design of Structures*, Vers.12, CSI, Berkeley, California.

[13] Mander J.B., Priestley M.J.N. and Park R. (1988). Theoretical stress-strain model for confined concrete, *Journal of Structural Engineering*, ASCE, 114(8), 1804-1826.